Composites Science and Technology 171 (2019) 62–69

Contents lists available at ScienceDirect

Composites Science and Technology

journal homepage: www.elsevier.com/locate/compscitech

DLC-treated aramid-fibre composites: Tailoring nanoscale-coating for macroscale performance

M. Kanerva[a,*], S. Korkiakoski[b], K. Lahtonen[c], J. Jokinen[a], E. Sarlin[a], S. Palola[a], A. Iyer[d], P. Laurikainen[a], X.W. Liu[d], M. Raappana[c], S. Tervakangas[e], M. Valden[c]

[a] Tampere University of Technology, Laboratory of Materials Science, PO Box 589, FI-33101, Tampere, Finland
[b] Aalto University, School of Engineering, Department of Mechanical Engineering, PO Box 14300, FI-00076, Aalto, Finland
[c] Tampere University of Technology, Laboratory of Photonics, PO Box 692, FI-33101, Tampere, Finland
[d] Aalto University, School of Chemical Engineering, Department of Chemistry and Materials Science, PO Box 14300, FI-00076, Aalto, Finland
[e] DIARC-Technology Oy, Kattilalaaksontie 1, FI-02330, Espoo, Finland

ARTICLE INFO

Keywords:
Aramid fibre
Interfacial strength
Photoelectron spectroscopy (XPS)
Finite element analysis (FEA)
Damage tolerance

ABSTRACT

This work aims to quantify the effect of a diamond-like carbon coating (DLC) treatment of aramid fibres and to reveal the conversion of a fibre-level performance leap on the macroscale mechanical behaviour. The DLC-based coating is applied directly to the reinforcement and laminates are infused with an epoxy matrix. After characterisation of the coated surfaces, the performance of the composite is analysed via interlaminar shear testing, fatigue testing and damage tolerance testing, microbond tests, and 3D finite element simulation using a cohesive zone model of the interface. The results show that the coating treatment improves the fatigue life and the S-N curve slope for the laminates, while the residual strength after impact damage and environmental conditioning (water immersion at 60 °C) remains high. The scaling factor to convert the performance on macroscale was determined to be 0.17–0.39 for the DLC-based fibre treatment.

1. Introduction

Aramid fibre reinforced plastics (AFRPs) are superior to carbon and glass fibre composites, not only in ballistic applications. AFRPs also have very low electrical conductivity, chemical inertness and high thermal resistance [1,2]. However, the interlaminar strength of AFRPs tends to be low. The underlying cause of low interfacial strength is the low adhesion of aramid fibres with essentially all traditional matrix polymers and the weak skin of the fibres themselves [3,4]. The challenge in modifying aramid fibre surfaces is that the chemical surface treatments, often being based on acidic solutions, damage the fibre bulk and lead to impaired mechanical behaviour [5,6]. Moreover, increased adhesion between fibres and matrix does not necessarily lead to increased impact resistance but vice versa [7]. The solution to these issues is to use an optimized, strong, and well adhering superficial layer. Instead of high-priced test programmes with different length scales, a procedure of microscale testing and modelling must be established to determine the scaling of the performance improvement on a nanoscale towards parameters on a macroscale, such as strength, fatigue life, and damage tolerance.

One of the methods with the most potential for optimizing the compatibility of aramid is the application of carbonous nanostructures on the fibre surface [8–10]. Diamond-like coatings (DLCs) in general are tough, stiff and strong, and they adhere well on different substrates: recent studies have shown that optimised DLC compounds can also introduce durable bonding with carbon nanotube networks [11,12] as well as adhesive polymers [13,14]. If the surface of aramid fibres could be strengthened by a strong coating and simultaneously improved in terms of the matrix-fibre adhesion, the application range of these composites will be widened enormously.

This work aims to enhance the potential of DLC-coated microscale fibres and laminate response. A coating treatment is applied to aramid fibre reinforcement and laminate structures are prepared using infusion of epoxy resin. The quality of the coating as well as the AFRP composite is analysed, whereafter the mechanical performance of the laminates is studied via interlaminar shear strength testing, fatigue testing, damage tolerance testing, microbond tests and finite element modelling. The results reveal the relation between the adhesion improvement and laminates' quasi-static as well as dynamic, fatigue performance.

* Corresponding author.
E-mail address: Mikko.Kanerva@tut.fi (M. Kanerva).

https://doi.org/10.1016/j.compscitech.2018.11.043
Received 23 February 2018; Received in revised form 20 June 2018; Accepted 25 November 2018
Available online 30 November 2018

Table 1
Procedure for washing reinforcement (sizing) prior to the coating treatment.

Step	Action	Medium
1	Ultrasonic cleaning (50 °C, 10 min)	Tap water
2	Ultrasonic cleaning (30 °C, 10 min)	Ethanol
3	Ultrasonic rinsing (50 °C, 5 min)	Purified water (Millipore Elix 10)
4	Dehydration in vacuum oven (70 °C, 14 h, 0.5 bar)	Air

2. Materials and methods

2.1. Reinforcement, coating and lamination

We used commercial aramid-fibre (Twaron® 2200 1210 dtex, Teijin) reinforcement from a single batch and with a 2/2 twill weave, an areal weight of 173–175 g/m^2 and with an areal bundle distribution of 50/50 in the 0° and 90° direction, respectively. The reinforcement for the laminates with a treatment was coated by DIARC-Technology Oy (Finland). A sheet of reinforcement was coated on one side at a time by commercial carbon-based coating DIARC® Bindo. In the DIARC plasma coating process, the part is treated in a vacuum at a low temperature below 100 °C. Carbon ions with high kinetic energy form a thin (from nanometres to micrometres) well adherent amorphous nanostructured coating when they hit the surface. Prior to the coating process, a series of the reinforcement samples were washed using a procedure, given in Table 1, to remove the processing finish (AT81).

The resin used for preparing AFRP composite laminates was a room-temperature-curing novolac epoxy resin (Araldite LY 5052, Aradur 5052, Huntsman International) mixed using a hardener-resin ratio of 38% (weight/weight). Laminates with a stacking sequence of $[0^\circ_{12}]$ and $[0^\circ_6]$ were manufactured on a mould by using the vacuum infusion technique (vacuum pressure 0.5 bar) for interlaminar shear strength testing and fatigue testing, respectively. The laminates for fatigue testing (nominal thickness 1.5 mm) were cured in the mould after infusion under vacuum pressure of 0.3 bar for 24 h at room temperature.

2.2. Characterisation

2.2.1. Raman spectroscopy

The coating on the aramid filaments was studied using a Raman spectroscope (LabRAM HR, Jobin Yvon Horiba) system using an Argon laser (λ= 488 nm; power = 4 mW on sample) with a BX41 (Olympus) microscope and 50×/10× objective. Samples of reinforcement (≈ 1 cm × 1 cm) were analysed directly without further preparation. For data comparison, linear background extraction was applied and curves were matched at 50 cm^{-1}.

2.3. X-ray photoelectron spectroscopy (XPS) and X-ray Auger electron spectroscopy (XAES)

The DLC nature of the coating (sp^2/sp^3 ratio) was examined using an electron spectrometer (Argus, Omicron Nanotechnology GmbH) utilising non-monochromatic Al Kα X-rays at 300 W. Data was recorded at normal emission with a detection area of 2.93 mm^2. The XPS C 1s C–C/H and sp^3 peaks were calibrated to 285.0 eV. The sp^2/sp^3 peak fitting was performed using component energy separation of 0.8 eV and proper Gaussian-Lorentzian line shapes of GL(90) tail(1.5) for sp^2 and symmetrical GL(80) for sp^3. In addition, the XAES C KLL transition was recorded to analyse the sp^2/sp^3 ratio also from the D-parameter [15] defined by the energy separation between minima and maxima in a differentiated C KLL spectrum. Samples were cut from the coating-treated and untreated reinforcement. To preserve the 0°/90° weave and neat fibre bundles given the relatively large analysis area, the sample edges (≈ 1 cm × 1 cm) were bonded using DP190 two-component epoxy (3M).

2.3.1. Contact angle measurement

Contact angle measurements were planned in order to estimate the effect of the coating treatment on wettability. For initial assessment, 5 μL droplets of purified water and diiodomethane (DIM) were placed directly on untreated (cleaned) and coating-treated aramid reinforcement. The device used was a model DSA100 (Krüss).

2.3.2. Imaging

Visual light microscopy (DM 2500 M, Leica) and scanning electron microscopy (SEM) using a field-emission gun electron microscope (ULTRAplus, Zeiss) were used for studying the fibre surfaces and polished laminate cross-sections. The samples after microbond tests were imaged directly without removing the samples off the microbond sample holder (after carbon evaporation). The nanoscale surface morphology was studied by using atomic force microscopy (AFM). Filament bundles were extracted from untreated and coating-treated reinforcement fabric and attached on metal chips at two points. The imaging was done by using a Dimension 3100 (Veeco/Bruker) apparatus in clean room conditions. Silicon tips (Nanosensors™) were used and the measurements were carried out in a tapping mode at a constant (0.21 Hz) scan rate. Height, amplitude, and phase-difference data were collected. The post-processing of data was done by rotating the data to align fibre longitudinal axis, printing of transverse-fibre profiles, and extraction of parabolic background to visualise the nanoscale details.

2.3.3. Nanoindentation

Nanoindentation and nano-scratch were performed to study the mechanical state and interfacial strength of the fibre-DLC coating interfaces on cross-sectioned AFRP laminate. A TI-900 TriboIndenter (Hysitron Inc.) testing system was used in the study. Based on the information from SEM observation and trial-indentation, the measurements were conducted under a load-control mode with a constant force of 200 μN and 50 μN for the indentation and scratch, respectively. Considering the rough cross-section surface and softness of the fibre, a spherical indenter (0.5 μm nominal tip radius) was selected to avoid excessive ploughing and material pile-up.

2.4. Mechanical testing

2.4.1. Fibre tenacity

The possible effect of the coating on the aramid fibre filaments' stiffness and strength was studied using a filament tester (Favigraph, Textechno) with 100 cN load cell and automatic filament gripping and testing. A gauge length of 20 mm and pre-tension of 0.60 cN/tex was applied. The tests were carried out at a 20 mm/min displacement rate in a standard environment; 100 samples were analysed. Stresses were calculated based on nominal (circular) cross-section confirmand via SEM and nanoindentation.

2.4.2. Interlaminar shear strength tests

Interlaminar shear strength (ILSS) tests and fatigue tests were performed using a universal test machine (Dartec, 100 kN) with computerised control (Elite Suite, MTS). ILSS tests were performed for water cut specimens (3 mm × 8 mm × 20 mm) in a three-point bend fixture (14 mm span) according to ASTM D2344 (displacement rate 1.0 mm/min) for dried and conditioned (wet) specimens. The wet specimens were immersed in distilled water (65 °C) for a week prior to testing; the dry specimens were dehydrated in a vacuum oven (50 °C, 0.5 bar) until they achieved constant weight [16]. For the wet specimens, three specimens per series were tested. Average shear stress values were calculated for six and three specimens for the dry and wet series, respectively.

2.4.3. Fatigue tests

The laminates were post-cured in an oven for 15 h at 60 °C and

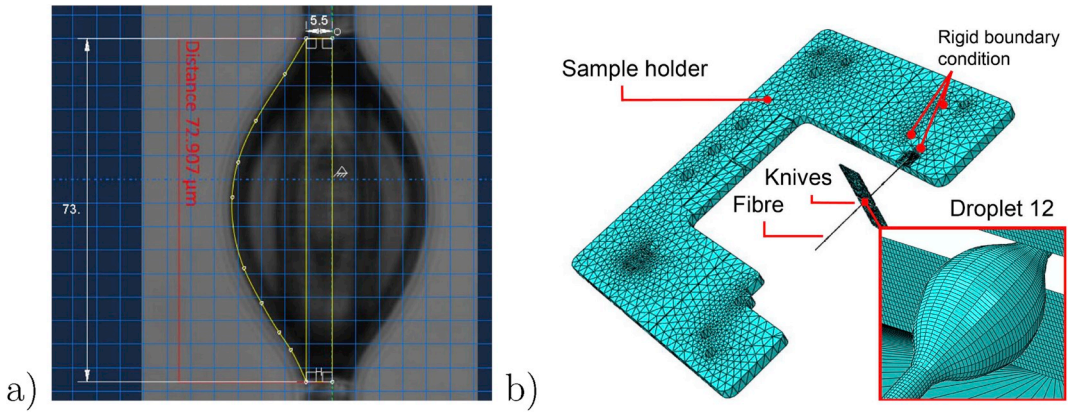

Fig. 1. FE modelling of fibre droplet samples and the test setup: (a) droplet modelling based on a microscopy image; (b) the FE model of the entire micro-droplet test setup.

water-cut, dog-bone shaped [17] specimens were prepared for the fatigue tests. The specimens were provided with glass fibre-reinforced epoxy (GFRE) tabs, bonded adhesively as described in previous studies [17]. Initial tensile moduli were measured prior to fatigue loading for all the specimens using a 50 mm extensometer and 7 kN/min load rate (stress-strain curve fit over 0.001–0.003 m/m range). A constant-load amplitude, sinusoidal wave-form uniaxial tensile loading with a stress ratio of R = 0.1 was applied for fatigue testing. A test frequency of 4 Hz was used to avoid excessive accumulation of heat. The fatigue test results were analysed as stress-number of cycles (S-N) graphs and the relationship between the maximum stress and the number of cycles to failure was formed using a power-law regression $N = C{\cdot}S^m$; the thickness and width measured at the specimen's gauge section, at three different points, were used to calculate averaged cross-sectional area and further the engineering stress (S). Here, the least-squares method was used according to ASTM E 739 to obtain parameters C and m; the number of cycles was used as a dependent variable.

2.4.4. Damage tolerance assessment

The damage tolerance assessment aimed to reveal the resistance of the laminates with coating-treated and untreated reinforcement against impact loads and subsequent ageing in a harsh environment. Rectangular specimens (27 mm × 170 mm, gauge length 110 mm) were water-cut from the laminate used for the fatigue test specimens. The specimens were provided with adhesively bonded GFRE tabs, in a similar way to the fatigue specimens. Two series (coating-treated/untreated) of impact-damaged specimens were produced by subjecting an impact (0.5 J–8.9 J) per specimen using impact apparatus according to ASTM D 5628-10 and a 15.9 mm spherical impactor. A carbon fibre-reinforced epoxy backing plate with a 25 mm hole for impact point and mechanical clamps were applied to give proper support to the specimen. After the impact loading, the specimens were immersed in distilled water and placed in an environmental chamber (60 °C) for four weeks. Finally, the specimens were tested using a universal tester (see Section 2.4.2) at a 7 kN/min loading rate and in wet conditions (each specimen removed from water immersion within two minutes before the test start). The residual strength of each specimen was determined based on the intact (net) cross-section and peak load. The quality of the intact specimens as well as the damage size per specimen after impact were determined using ultrasonic inspection prior to impact loading, after impact loading and after the water immersion. Ultrasonic inspection device (Omniscan MX, Olympus) was used in a transmission (2.25 MHz) mode and inspection operated under water.

2.4.5. Microbond tests

The adhesion between the matrix and single fibres was studied using a FIBRObond micro-droplet tester [18]. Here, the tester was set to use a 1 N load cell, surgeon knives (R35, thickness 0.254 mm, Feather, Japan) for droplet loading, and an electrical linear motor to load the droplet. The droplets were prepared using a developed resin dip method with the same resin batch as for the laminates (Section 2.1). Coating-treated filaments were extracted from the outer surface of the reinforcement bundles. The droplet fibre samples were cured in an oven (50 °C) for 18 h. Droplets of different sizes were prepared to observe the effect of droplet size on the ultimate, peak force. The tests were performed at a constant displacement rate until detachment of the droplet, and the peak force and embedded area were used to calculate interfacial average shear strength (IFSS).

2.5. Interface modelling

The interface between the fibres and the matrix was modelled on a finite element (FE) basis using Abaqus® 2017, standard (Dassault Systèmes). The target was to form a mechanical model of the interface that covers the elastic behavior and damage. The 3D geometry of untreated and coating-treated fibre droplet samples were modelled based on their microscopy images (Fig. 1) and the rest of the test setup was modelled to account for the overall deformation. The sample holder was meshed using quadratic elements (C3D10) and the rest of the system using linear tetras (C3D4), wedges (C3D6) and bricks (C3D8R). The sample holder was modelled as linear cast acrylic (Young's modulus 3.3 GPa, Poisson's ratio 0.35), the surgeon knives as linear steel (modulus 210 GPa, Poisson's ratio 0.3), fibre as linear aramid (Young's modulus 108 GPa, Poisson's ratio 0.3), and the resin droplet as initially linear epoxy following ideal plastic yield (Young's modulus 3.2 GPa, Poisson's ratio 0.35, yield stress 84 MPa, ultimate strength 86 MPa at 0.09 m/m plastic strain). Residual stresses due to the cure at elevated temperature were included applying a linear thermal expansion of 71 µm/(m K) and 37 µm/(m K) for the epoxy and aramid, respectively, and thermal loading of ΔT = −30 °C (cool-down), by using a separate step in the finite element analysis (FEA).

The fibre matrix interface was modelled using cohesive zone (CZM) elements with a bilinear traction-separation law, initial stiffness of 10^{15} N/m^3 for all three fracture modes, and the following damage onset criterion:

$$max\left\{\frac{\tau_{1,ap}}{\tau_c}, \frac{\tau_{2,ap}}{\tau_c}, \frac{\tau_{3,ap}}{\tau_c}\right\} = 1\ , \tag{1}$$

where τ is traction, sub-indices *1, 2, 3* refer to the fracture modes (mode I, mode II, mode III, respectively), *ap* to a momentary value per applied load level, and *c* to a critical value. Interfacial damage evolution was given a critical energy release rate limit, G_{cr}, to define full debond at the interface. The crack-tip mode mixity upon crack propagation was taken into account using a linear interaction law:

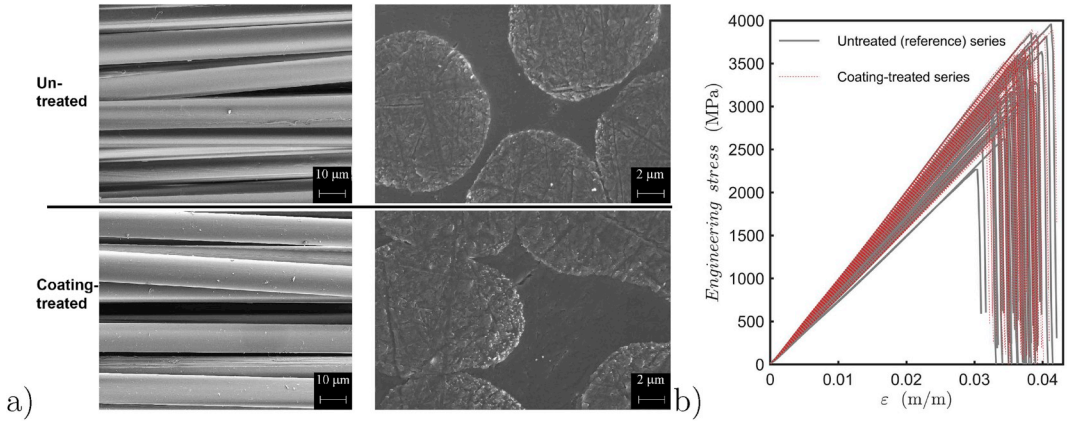

Fig. 2. Fibre characterisation: (a) force-extension curves; (b) SEM of untreated and coating-treated fibres, and cross-sections of the fibres in laminates.

$$f = \frac{G_I}{G_{cr}} + \frac{G_{II}}{G_{cr}} + \frac{G_{III}}{G_{cr}}, \quad (2)$$

where G is energy release rate, and sub-indices *I, II, III* refer to the fracture modes.

3. Results

3.1. Fibre and coating characterisation

The SEM imaging indicated that the DLC coating-treated fibre surface was smooth and was well wetted by the resin in the laminate (Fig. 2(a)). The fibre testing resulted in an average ultimate load of 0.313 ± 0.094 N and 0.320 ± 0.096 N (i.e. ≈3370–3290 MPa) for the untreated and coating-treated fibres, respectively (full curves in Fig. 2(b)). Clearly, the coating resembled nanoscale surface treatment and did not affect the bulk fibre behavior significantly. Overall, the ultimate stress level is of the order of high-strength aramid fibres, such as Kevlar 49® (DuPont). The SPM (scanning probe microscopy) imaging and nanoindentation data confirmed a filament diameter of ≈11 µm and also clean, well-wetted interfaces in the epoxy-infused laminates, as shown in Fig. 4(a). The Raman spectra for coating-treated and untreated filaments are shown in Fig. 4(b), where the reference spectra show typical output for aramid surface [19,20]. Analysis of the DLC character on the coating-treated fibres was deemed unreliable due to the DLC hump [12,21] overlapping with the aramid peaks.

The surface morphology of untreated and coating-treated single filaments was studied by using AFM (see Fig. 3). The vacuum deposition method applied for the coating, resembling a kind of hybrid between chemical and physical vapour deposition, forms a slightly more rough surface compared to the reference, untreated fibres. It should be noted that, due to coating fabric instead of fibres, the coating thickness, as well as the surface structure vary locally. Therefore, the imaging, such as in Fig. 3(b), represents only local, nanoscale roughness on the surface.

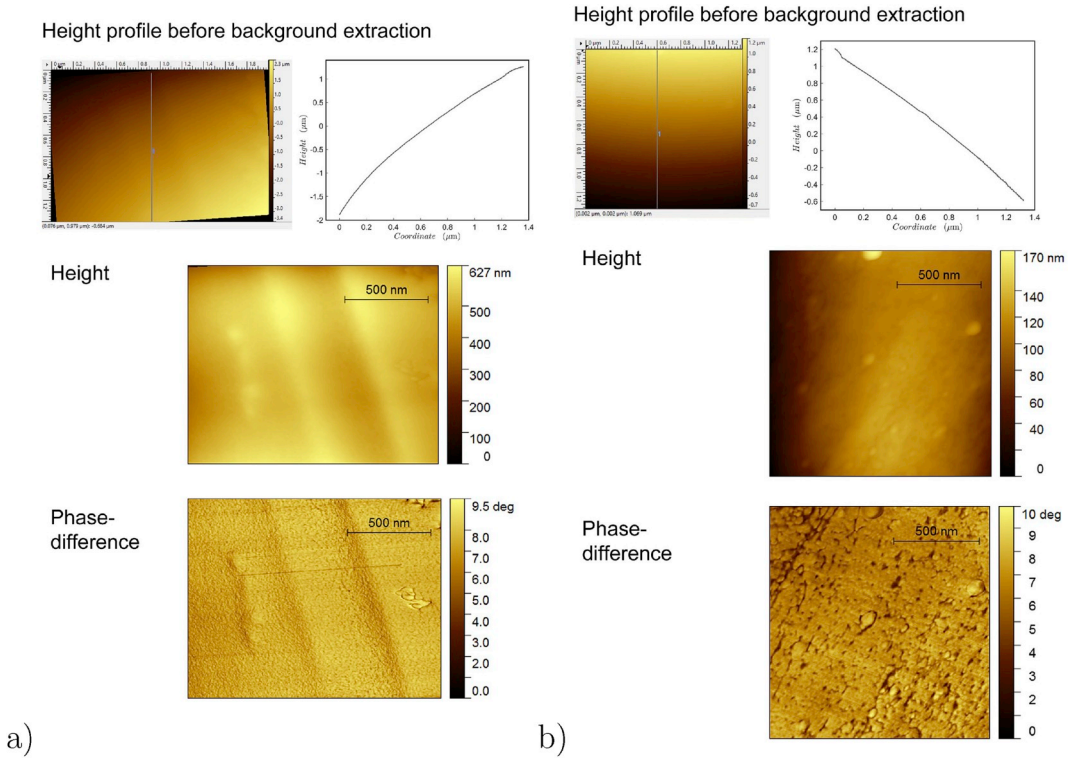

Fig. 3. AFM analysis of fibres: (a) untreated filament surface; (b) coating-treated filament surface. For all data shown, the fibre longitudinal axis runs approximately in the horizontal direction.

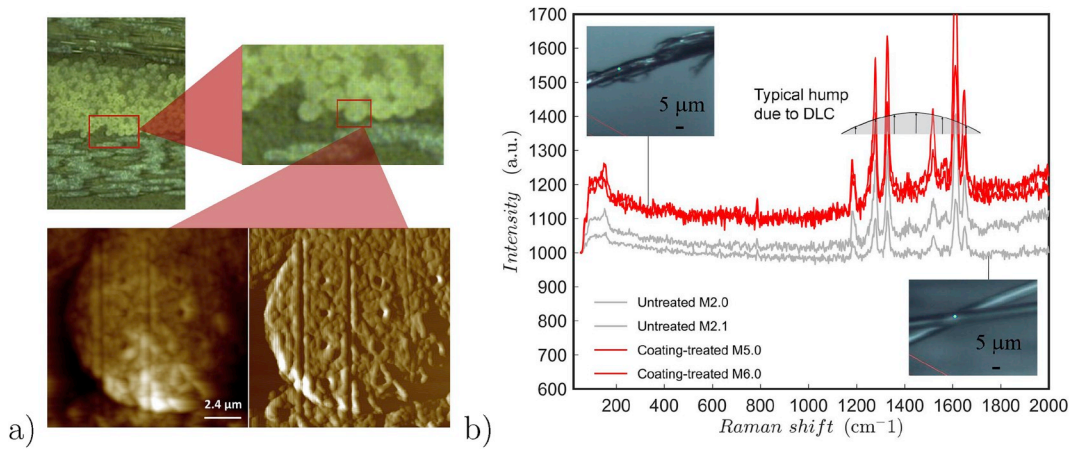

Fig. 4. Coating characterisation: (a) nanoindentation on coating-treated reinforcement; (b) typical Raman spectra of untreated and coating-treated reinforcement.

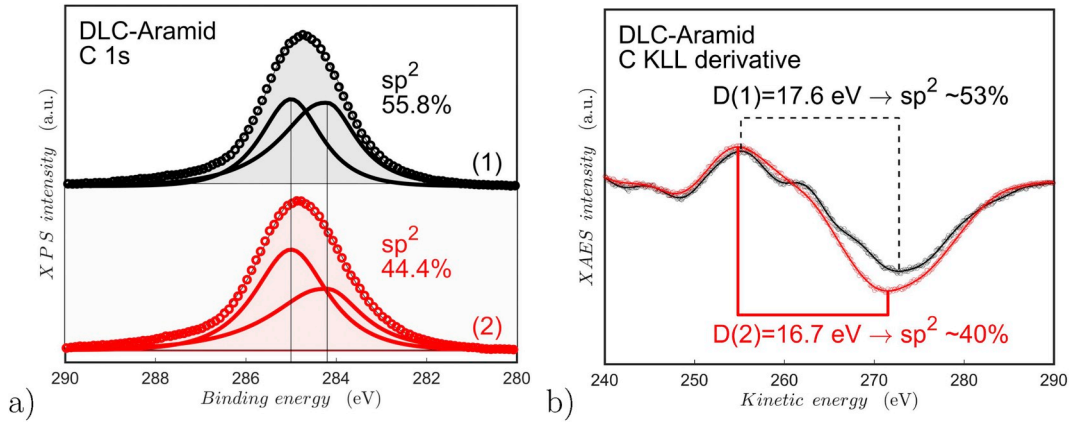

Fig. 5. XPS/XAES analysis of the coating-treated reinforcement surface from two distinct measurement positions showing typical spectra and variation observed on the surface: (a) C 1s peak and fit; (b) derivative of the C KLL spectrum and determination of the D-parameter value.

The DLC coating on the aramid filaments was further analysed based on XPS/XAES data of the coating-treated reinforcement surface. The C 1s peak and the 1st derivative of the KLL region HR spectra are shown in Fig. 5. Pure diamond (ta-C type) coatings are based on the sp^3 carbon bond whereas graphite represents pure sp^2 bonding (a:C type). Here, the analysis of the two synthetic components of the C 1s fit yielded a semi-quantitative [21] sp^2 content of 44–56% for the coating surface. The interpretation of the D-parameter in turn supported a sp^2 content of 40–53% verifying that the DLC coating had a significant sp^3 fraction. In general, the properties of DLC coatings can be adjusted by process parameters, and the sp^3/sp^2-ratio optimised per application; values of 50–100% being typical [21].

The surface wettability for polar and nonpolar liquids (water, DIM) was observed to be very good. It was not possible to measure droplet contact angles due to the droplets were instantly absorbed into the reinforcement (Fig. 6)—suggesting a high surface energy level for untreated and coating-treated fibers.

3.2. Mechanical performance of laminates

The ILSS values for the laminates with either coating-treated or untreated reinforcement are shown in Fig. 7(a). The washing process

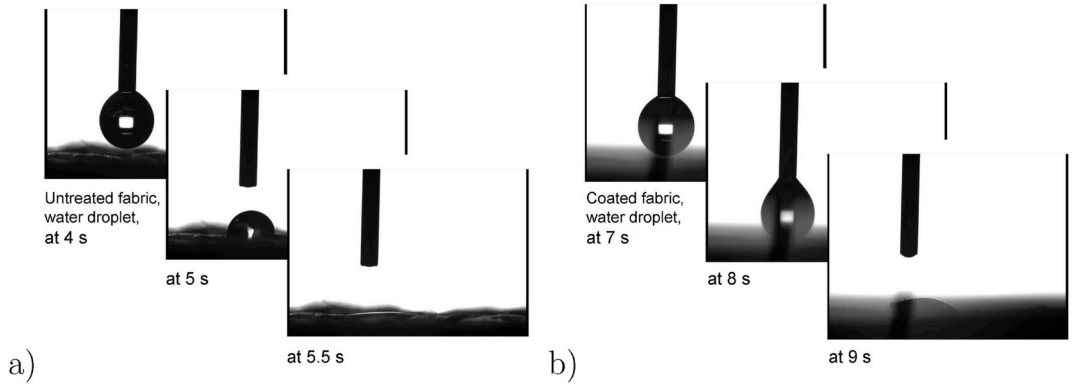

Fig. 6. Contact angle study directly on fabrics: (a) untreated (washed) fabric; (b) coating-treated fabric.

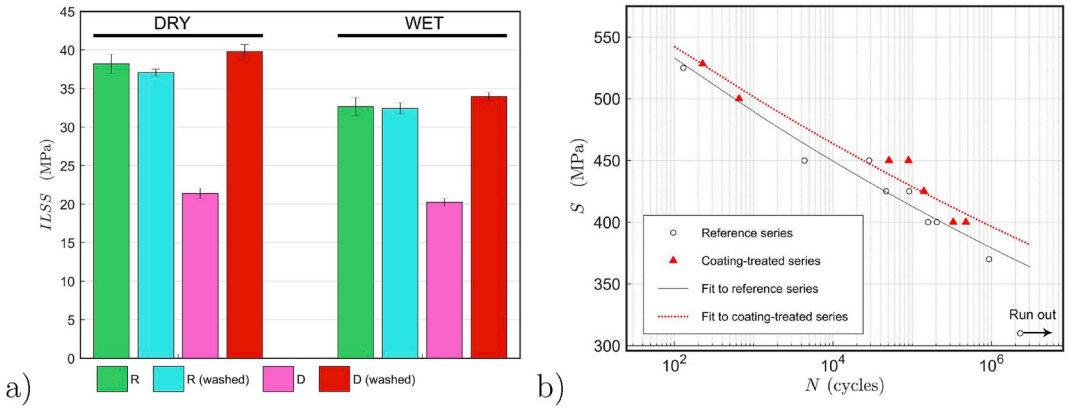

Fig. 7. Mechanical testing results: (a) average ILSS results (R = untreated series, D = coating-treated series); (b) fatigue data and determined S-N curves.

significantly affected the coating-fibre compatibility—washing increased the ILSS value by 86% (dry state) for the coating-treated laminates, whereas the effect of washing was negligible in the untreated case. The average ILSS for the coating-treated samples with the washing process was found to be 4.0–4.2% higher compared to the fully untreated samples, depending on the test conditions (dry/wet). The ILSS values for both the reference laminates and the coating-treated laminates with the washing process (Table 1) were 20–43% higher than reported values in the current literature for H_3PO_4 and bromination treated aramid-epoxy laminates [6,22].

Fatigue of composites in general is sensitive to fibre surface treatments and can reveal any underlying potential to strengthen aramid-epoxy interfaces. The fatigue test results are shown in Fig. 7(b) and it can be seen that the fatigue lives significantly improved throughout the applied stress range due to the coating treatment. The slope parameter of the S-N curve fit resulted in values of −25.47 and −27.80 for the untreated and coating-treated laminates, respectively. The initial Young's moduli indicated slightly higher values for the coating-treated specimens (29.72 ± 0.9 GPa) compared to un-treated specimens (28.03 ± 0.5 GPa)—yet the difference is within experimental scatter due to measured laminate thickness variation. The ultrasonic inspection results (Fig. 8(a)) for the damage tolerance analysis revealed greater damage per impact energy for the laminates with coating-treated reinforcement. However, based on the damage tolerance tests, the residual strength of the coating-treated laminate specimens after impact and water exposure remained the same or was higher (+9.4 ± 5%, 0–2.2 J impacts) throughout the impact energy range compared to the untreated specimens (Fig. 8(b)). In the current literature, improved in-plane mechanical properties of aramid-epoxy laminates due to any fibre treatment have led to impaired impact properties [7,22].

3.3. Interface strength and model parameters

The results of the microbond tests are shown in Fig. 9(a). Based on the peak forces and individual embedded areas of droplets, statistical IFSS values of 17.6 ± 3.6 MPa and 21.7 ± 5.2 MPa were calculated for the untreated and coating-treated samples. The results indicate improvement in adhesion (≈24%) with the coating treatment. FEA was carried out to validate the experimental IFSS values; the fitted response compared to raw force-displacement data is shown in Fig. 9(b). The fitting resulted in model parameters of τ_c = 22.7 MPa and G_{cr} = 650 J/m^2 for the untreated filament droplet sample, and τ_c = 22.2 MPa and G_{cr} = 500 J/m^2 for the coating-treated filament droplet sample (respective IFSS values 21.7 MPa and 20.3 MPa). These results establish the validity of microbond IFSS values to be used in the determination of the onset criterion for the developed interface model. The fitted traction values are realistic when compared to the microbond tests and reported interfacial stress values related to failure—although direct comparison with the reported simulations cannot be made due to the simplified non-3D (axisymmetric) models in the current literature, e.g. by Nishikawa et al. [23] and Sato et al. [24].

The samples were imaged after testing, and typical fracture surfaces are shown in Fig. 10. The imaging reveals a skin-like layer on the fracture surface of the coating-treated samples and it might resemble the DLC coating. Skin-like, torn strips are also shown on the fracture surfaces of untreated samples but they can be shredded bulk filament surface. In general, based on AFM and SEM images, the surfaces of the untreated fibres often contain grooves and torn off-pieces. Our hypothesis is that the coating might form a protective layer preventing fracture of the bulk fibre surface. Additionally, the sharp-edged grooves on untreated filaments might work as stress concentration points and

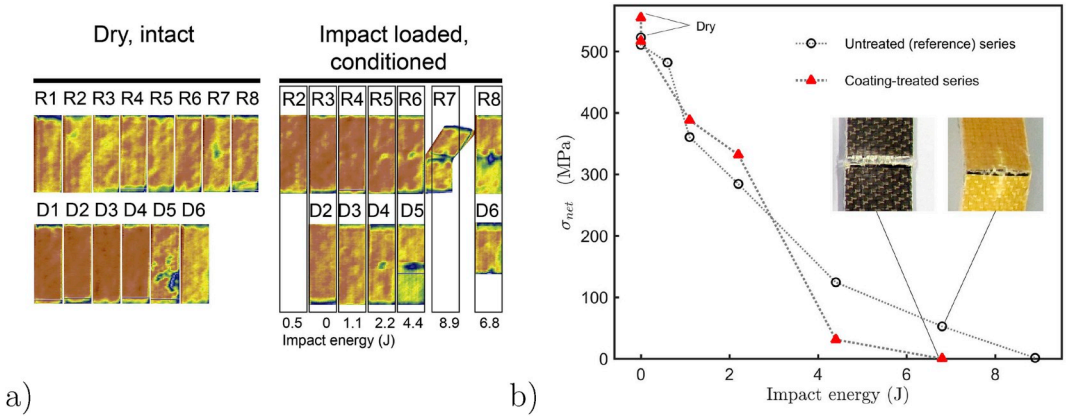

Fig. 8. Damage tolerance analysis: (a) ultrasonic inspection of the test specimens before and after impact and conditioning (R*i* = untreated series, D*i* = coating-treated series); (b) residual strength after impact and conditioning.

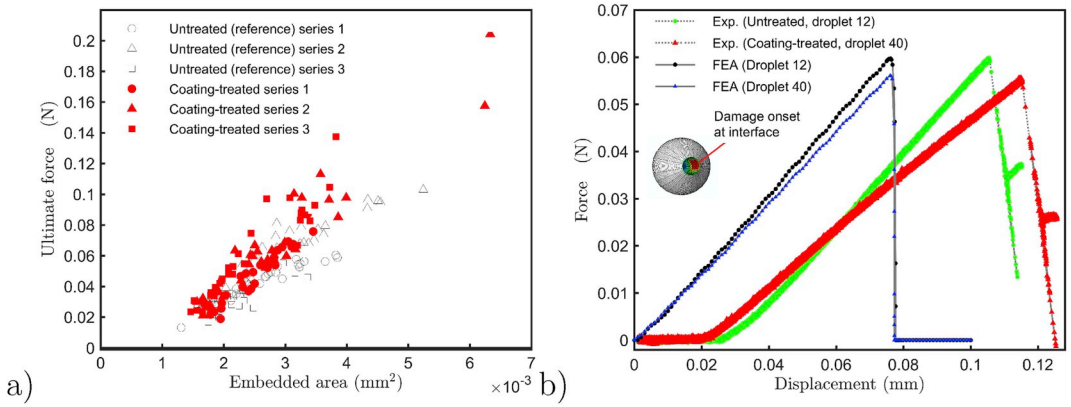

Fig. 9. Microbond test results and interface simulation: (a) test results; (b) representative FEA results for untreated (droplet 12) and coating-treated (droplet 40) tests.

lead to premature interfacial failure on untreated filaments.

4. Discussion

The direct effect of a surface treatment for fibres is defined by the interphase formed when embedded by a matrix. Here, a 3D crack propagation model was fitted for fibre-matrix interfaces based on force-displacement data from microbond tests. The determined traction limit τ_c of damage initiation at the untreated and coating-treated interfaces verified the applicability of bare IFSS values —typically derived based on pure microbond test data. The modification of aramid fibre interface must be optimised per application, and the surface treatment can evidently be adjusted using the microbond test. Furthermore, a fitted interface model can be applied to describe the interfacial performance for larger models, representative volume elements (RVEs), and sub-models for structural design [24,25]. Thus, for industrial applications, optimisation of the DLC coating for aramid fibre reinforcements can be carried out faster and at markedly lower costs using the microbond-FEA procedure prior to coupon and certainly before component-level testing. Due to the nature of microbond tests [26,27], hundreds of tests are needed to achieve reliable statistical significance, which formerly has not been possible. Finally, what is essential is how much the adhesion at fibre matrix interfaces must be improved to gain a certain enhancement on the macroscopic performance, such as strength and fatigue life. In this study, the IFSS values supported by FEA suggested an adhesion enhancement of 24% on the fibre level. Scaling factor values of 0.17, 0.38 and 0.39 must be then applied to estimate the observed improvement in ILSS (4% improvement), S-N curve slope (9.14% improvement) or residual strength after low energy impact and conditioning (9.4% improvement), respectively. The scaling factor gives a convenient indication of the transfer of the benefits of fibre-matrix adhesion and it clearly establishes the significance of the nanoscale surface treatment on aramid fibres.

The mechanism of interfacial strengthening by the DLC coating was concluded to occur via protection or strengthening of the bulk fibre surface, in addition to strong adhesion to the epoxy matrix; the coating-matrix interface was assessed to be the point of failure initiation during the microbond tests. Similar defect-covering characteristics for surface treatments of carbon-fibres have been reported in the current literature [28,29].

5. Conclusions

In this study, aramid-fibre fabric was directly treated on its outer surfaces using a DLC-based coating and composite laminates were prepared with epoxy resin using vacuum infusion. The experimental results of the characterisation and laminate testing confirmed the following: in the case of coating treatment, the ultrasonic washing process of the aramid reinforcement improved the interlaminar shear strength (ILSS) by 86%. The ILSS of the laminate with the wash and coating treatment on the reinforcement was comparable or better (≈4%) compared to the untreated laminate with off-the-shelf reinforcement in both dry and wet conditions. For the coating-treated laminates, the slope parameter of the S-N curve fitted to the tensile-tensile fatigue data improved by 9.14% compared to the results of the untreated laminate. Also, the residual static strength after conditioning (water immersion at 60 °C) and moderate impact (0–2.2 J) was on average 9.4 ± 5.0% higher for the coating-treated laminate compared to untreated

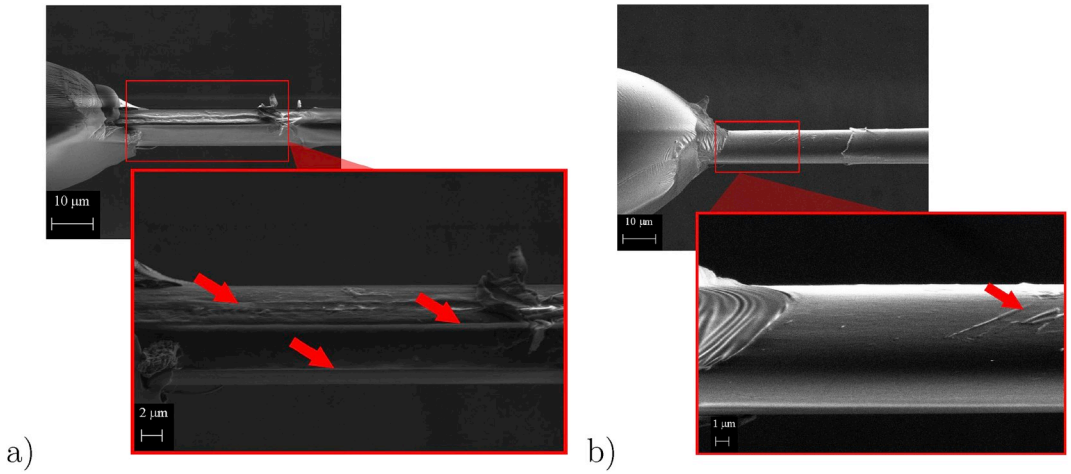

Fig. 10. Fracture surfaces after microbond tests: (a) untreated filament-droplet interface; (b) coating-treated filament-droplet interface.

laminate, suggesting improved damage tolerance. The results show that an optimised surface treatment can improve the overall performance of aramid fibre reinforced structures. Moreover, the finite element simulations and microbond tests revealed that the scaling of the filament-level adhesion improvement is less than unity to reach the macroscale effect: in the case of the DLC-based coating and the aramid-epoxy laminate, the scaling factor was 0.17–0.39 depending on the parameters on a macroscale (ILSS, S-N curve slope, residual strength after impact).

Acknowledgements

This investigation was funded by a grant from the Finnish Metals and Engineering Competence Cluster (FIMECC HYBRIDS) and by the HISCON (259595) project from Academy of Finland. Authors acknowledge Kevra Oy and researchers H. Niemelä-Anttonen and M. Kakkonen for assistance with experimental activities.

References

[1] S. Luo, W. Van Ooij, Surface modification of textile fibers for improvement of adhesion to polymeric matrices: a review, J. Adhes. Sci. Technol. 16 (13) (2002) 1715–1735.
[2] K. Imielińska, L. Guillaumat, The effect of water immersion ageing on low-velocity impact behaviour of woven aramid–glass fibre/epoxy composites, Compos. Sci. Technol. 64 (2004) 2271–2278.
[3] P. de Lange, P. Akker, E. Mäder, S.L. Gao, W. Prasithphol, R. Young, Controlled interfacial adhesion of Twaron aramid fibres in composites by the finish formulation, Compos. Sci. Technol. 67 (10) (2007) 2027–2035.
[4] P. Tarantili, A. Andrepoulos, Mechanical properties of epoxies reinforced with chloride-treated aramid fibers, J. Appl. Polym. Sci. 65 (1997) 267–276.
[5] T. Lin, S. Wu, J. Lai, S. Shyu, The effect of chemical treatment on reinforcement/matrix interaction in Kevlar-fiber/bismaleimide composites, Compos. Sci. Technol. 60 (2000) 1873–1878.
[6] J. Lin, Effect of surface modification by bromination and metalation on Kevlar fibre-epoxy adhesion, Eur. Polym. J. 38 (2002) 79–86.
[7] M. Shaker, I. Kamel, F. Ko, J. Song, Improvement of the interfacial adhesion between Kevlar fiber and resin by using R-F plasma, J. Compos. Technol. Res. 18 (4) (1996) 249–255.
[8] D. Devlin, K. Hubbart, K. Siebein, T. Archuleta, D. Coates, Diamond like carbon coated Kevlar for improved mechanical properties, 13th ICCVD Conference; vol. 96. Electrochemical Society Proceedings, US, 1996, pp. 691–698.
[9] Devlin, D., Coates, D., Archuleta, T.. Diamond-like-carbon coated aramid fibers having improved mechanical properties. 2002. US Patent 6,432,537.
[10] S. Palola, E. Sarlin, S. Kolahgar Azari, V. Koutsos, J. Vuorinen, Microwave induced hierarchical nanostructures on aramid fibers and their influence on adhesion properties in a rubber matrix, Appl. Surf. Sci. 410 (2017) 145–153.
[11] H. Schittenhelm, D. Geohegan, G. Jellison, A. Puretzky, M. Lance, P. Britt, Synthesis and characterization of single-wall carbon nanotube-amorphous diamond thin-film composites, Appl. Phys. Lett. 81 (2002) 11.
[12] A. Iyer, A. Kaskela, L.S. Johansson, L. Xuwen, E. Kauppinen, J. Koskinen, Single walled carbon nanotube network—tetrahedral amorphous carbon composite film, J. Appl. Phys. 117 (22) (2015) 225302.
[13] J. Takahashi, A. Hotta, Adhesion enhancement of polyolefins by diamond like carbon coating and photografting polymerization, Diam. Relat. Mater. 26 (2012) 55–59.
[14] J. Aakkula, J. Jokinen, O. Saarela, S. Tervakangas, Testing and modelling of Diarc plasma coated elastic plastic steel wedge specimens, Int. J. Adhesion Adhes. 68 (2016) 219–228.
[15] A. Mezzi, S. Kaciulis, Surface investigation of carbon films: from diamond to graphite, Surf. Interface Anal. 42 (2010) 1082–1084.
[16] J. Posio, Interlaminar Shear Strength Testing of Non-unidirectionally Reinforced Composites, M.Sc. thesis Aalto University, Finland, 2016.
[17] S. Korkiakoski, P. Brondsted, E. Sarlin, O. Saarela, Influence of specimen type and reinforcement on measured tension–tension fatigue life of unidirectional GFRP laminates, Int. J. Fatig. 85 (2016) 114–129.
[18] M. von Essen, E. Sarlin, O. Tanhuanpää, M. Kakkonen, P. Laurikainen, M. Hoikkanen, et al., Automated high-throughput microbond tester for interfacial shear strength studies, The SAMPE Europe Conference. Stuttgart, Germany, 2017,November, pp. 14–16.
[19] L. Penn, F. Milanovich, Raman spectroscopy of Kevlar 49 fibre, Polymer 20 (1) (1979) 31–36.
[20] H. Cen, Y. Kang, Z. Lei, Q. Qin, W. Qiu, Micromechanics analysis of Kevlar-29 aramid fiber and epoxy resin microdroplet composite by Micro-Raman spectroscopy, Compos. Struct. 75 (1–4) (2006) 532–538.
[21] X. Yan, T. Xu, S. Yang, H. Liu, Q. Xue, Characterization of hydrogenated diamond-like carbon films electrochemically deposited on a silicon substrate, J. Phys. D Appl. Phys. 37 (17) (2004) 2416–2424.
[22] S.J. Park, M.K. Seo, T.J. Ma, D.R. Lee, Effect of chemical treatment of Kevlar fibers on mechanical interfacial properties of composites, J. Colloid Interface Sci. 252 (2002) 249–255.
[23] M. Nishikawa, T. Okabe, K. Hemmi, N. Takeda, Micromechanical modeling of the microbond test to quantify the interfacial properties of fiber-reinforced composites, Int. J. Solid Struct. 45 (14) (2008) 4098–4113.
[24] M. Sato, E. Imai, J. Koyanagi, Y. Ishida, T. Ogasawara, Evaluation of the interfacial strength of carbon-fiber-reinforced temperature-resistant polymer composites by the micro-droplet test, Adv. Compos. Mater. 26 (5) (2017) 465–476.
[25] A. Hodzic, S. Kalyanasundaram, A. Lowe, Z. Stachurski, The microdroplet test: experimental and finite element analysis of the dependance of failure mode on droplet shape, Compos. Interfac. 6 (4) (1998) 375–389.
[26] Y. Hou, T. Sun, An improved method to make the microdroplet single fiber composite specimen for determining the interfacial shear strength, J. Mater. Sci. 47 (1) (2012) 4775–4778.
[27] M. Pitkethly, J. Favre, U. Gaur, J. Jakubowski, S. Mudrich, D. Caldwell, et al., A round-robin programme on interfacial test methods, Compos. Sci. Technol. 48 (1) (1993) 205–214.
[28] X. Zhang, X. Fan, C. Yan, L. Hongzhou, Y. Zhu, X. Li, et al., Interfacial microstructure and properties of carbon fiber composites modified with graphene oxide, ACS Appl. Mater. Interfaces 4 (1) (2012) 1543–1552.
[29] J. Dong, C. Jia, M. Wang, X. Fang, H. Wei, H. Xie, et al., Improved mechanical properties of carbon fiber-reinforced epoxy composites by growing carbon black on carbon fiber surface, Compos. Sci. Technol. 149 (1) (2017) 75–80.